EFDA–JET–CP(12)01/06

D. Marocco, B. Esposito, M. Riva
and JET EFDA contributors

Ion Temperature Profile Measurements at JET Using the Upgraded Neutron Profile Monitor

Ion Temperature Profile Measurements at JET Using the Upgraded Neutron Profile Monitor

D. Marocco, B. Esposito, M. Riva
and JET EFDA contributors*

JET-EFDA, Culham Science Centre, OX14 3DB, Abingdon, UK

Associazione EURATOM-ENEA sulla Fusione, C.R. Frascati, C.P. 65, Frascati I-00044, Roma, Italy
** See annex of F. Romanelli et al, "Overview of JET Results",*
(23rd IAEA Fusion Energy Conference, Daejon, Republic of Korea (2010)).

Preprint of Paper to be submitted for publication in Proceedings of the
High Temperature Plasma Diagnostics (HTPD) 2012, Monterey, California, USA.
7th May 2012 - 10th May 2012

ABSTRACT

The neutron profile monitor is routinely used at the Joint European Torus for neutron emissivity profile measurements. The diagnostic consists of two fan-shaped arrays of collimators and each line of sight is equipped with a NE213 liquid organic scintillator for simultaneous measurements of the 2.5MeV and 14MeV neutrons. The diagnostic has been upgraded by replacing its analog acquisition electronics with a digital system developed in ENEA. The new acquisition chain enables the NPM to perform spatially-resolved neutron spectrometry by providing neutron pulse height spectra for each LOS. However, the conditions for neutron spectrometry with the NPM are not optimal since this diagnostic was not originally designed as a spectrometer and therefore lacks several key features, such as detailed measurements of the detector response functions and the presence of detector stability monitors. In this paper, a proof of principle of ion temperature profile measurements derived from the NPM PHS in high plasma current discharges using simulated detector response functions are presented.

1. INTRODUCTION

The neutron profile monitor (NPM, Fig.1) has been in use at JET since 1986 as a diagnostic for the measurement of the 2.5MeV (DD) and 14MeV (DT) neutron emissivity profile [1].

The NPM consists of 2 concrete shields each of which includes a fan-shaped array of collimators. These collimators define a total of 19 lines of sight (LOS), grouped in two cameras. The larger one contains 10 collimated channels with an horizontal view through the plasma while the smaller one has 9 channels with a vertical view. The collimation can be adjusted by the use of 2 pairs of rotatable steel cylinders.

Originally, the NE213 scintillator detectors essentially worked as DD and DT neutron flux monitors above a selectable proton energy threshold based on analog Pulse Shape Discrimination (PSD) electronics [2]. The pulses from each detector were fed to a pair of analog PSD modules in which n/g separation and a rough neutron energy discrimination (only proton recoil events falling in a preselected energy band were recorded) were simultaneously performed. The energy bands of the two PSD units were respectively tuned to DD and DT neutrons and set on the basis of gamma calibrations performed through built-in ^{22}Na γ-ray sources.

In the frame of the JET diagnostic enhancement programme the NPM analog acquisition chain has been entirely replaced by a digital system developed in ENEA-Frascati [3]. The system enables the diagnostic to provide, for each LOS, the neutron pulse height spectrum (PHS) i.e. the convolution of the neutron spectrum measured along the LOS with the box-like shaped Response Functions (RF) of the scintillator. Unfolding techniques can be applied to recover the actual spectrum from the measured PHS.

The energy spectrum of the neutron emission from fusion plasmas depends on the underlying kinetics of the thermal and non-thermal velocity components of the fuel populations. Ions in thermal equilibrium produce Gaussian neutron spectra, while reactions between thermal and non-thermal ions produced by Radio Frequency/Neutral Beam Injection generate non-Gaussian neutron spectral components that vary with the orientation of the LOS with respect to the toroidal magnetic field. The unfolding of the NPM PHS and the extraction of the thermal spectral component can therefore

directly provide a measurement of the line-integrated ion temperature profile from the Doppler width of the Gaussian term: in the case of DD reactions the relation $\Delta E(FWHM) = 82.5 \times T^{0.5}$ (ΔE and T in keV) holds. Finally, as demonstrated for the nearly thermal ITER DT plasma using synthetic data [4], the local ion temperature profile can be retrieved by spatial inversion of the thermal components of the unfolded spectra.

The present paper reports on the first results of ion temperature profile measurements in JET using spectroscopic methods applied to the NPM. This analysis must be considered as a proof of principle, since the measurement is challenging for the following reasons:

a) Lack of RF knowledge: the accuracy of the unfolding heavily relies on the detailed knowledge of the detectors RF; experimentally determined response functions obtained by time of flight measurements are necessary to achieve high resolution ($\Delta E/E = 4\%$ at 2.5MeV and $\Delta E/E = 2\%$ at 14MeV, [5]). No measured RF are available for the NPM detectors.

b) Lack of Light Emitting Diode (LED) correction system: the measured PHS can be distorted due to changes of gain of the photomultiplier (PMT) coupled to the scintillators induced by changes in the rate of the incoming neutrons. This issue can be monitored and corrected using LED based systems in which the PMT is fed, together with the true signal, with a reference signal from an LED [6]. No such a system is available for NPM detectors.

2. MATERIALS AND METHODS

2.1. THE ACQUISITION SYSTEM ARCHITECTURE

The new NPM acquisition system consists of five acquisition boards with 4 acquisition channels each, for a total of 20 channels (1 spare). The sampling rate of each channel is 200 MSamples/s (14 bits) obtained combining two ADC @100MHz with a relative delay of 5ns. The boards are based on the Field Programmable Gated Array (FPGA) technology. The FPGA is programmed to acquire the scintillator signal non continuously, in discrete sets of samples (data windows); the size of the data windows varies dynamically, depending on the pulse duration and on the occurrence of other pulses during its acquisition. This Dynamic Window Data Acquisition technique (DWDA, [7]) allows to record only meaningful data and thus to increase the count rate capability of the system and to reduce the amount of stored data. Data processing is performed off line by a specifically developed LabView^{TM} code providing separate n/γ PHS and count rates [6]. For more details concerning the acquisition system refer to [3,6].

2.2. DISCHARGE SELECTION

The choice of the discharge for testing the NPM capability to measure the ion temperature profile was guided by the request of having a large thermal neutron emission, in order to minimize the effect of the uncertainties in the NPM spectrometric measurements: the best chance occurs for high current discharges in which the thermal component is expected to be large due to better confinement and thus higher temperature. Pulse No: 79698 ($I_p = 4.5$MA; $B_t = 3.6$T; $P_{NBI} = 22.9$MW; $P_{ICRH} = 2.6$MW; neutron rate $Y_N \sim 1.5 \times 10^{16}$ s^{-1}, $n_e = 1.2 \times 10^{20}$ m^{-3}) was therefore selected and analyzed in the stationary phase 12-16s in which a maximum total count rate of ~320kHz was recorded in the central vertical #15 LOS (see [3] for further details). Moreover, for this discharge detailed

[1] *The term unfolding is used here in a broad sense, indicating any technique capable of retrieving the energy spectrum from PHS measurements.*

measurements from the TOFOR neutron spectrometer (single vertical & central LOS) are available: line-integrated ion temperature $T_{TH\ TOFOR}$ ~ 6keV and thermal fraction (ratio of thermal to total neutrons) ~65% [8].

2.3. DATA ANALYSIS

The NPM data were analyzed following the procedure described in [4] consisting in the application of unfolding and spatial inversion algorithms to the measured PHS. The unfolding is performed using a forward convolution approach[1] in which a parametric model is assumed for the unknown line-integrated spectra; the model is folded with the RF and the difference between the measured and folded PHS is minimized using χ^2 statistics. Spatial inversion of the thermal component of the line-integrated spectra is carried out using a Tikhonov regularization algorithm applied energy bin by energy bin to the set of line-integrated spectra.

2.3.1. Response functions

A single set of 2685 RF simulated using the NRESP7 code [9] for a 1cm thick and 2cm diameter NE213 detector and for neutrons with energies between 1MeV and 19.5MeV was used for the unfolding of all NPM detectors. These RF, kindly provided by the Physikalisch-Technische Bundesanstalt (PTB, Braunschweig, Germany), might significantly differ from those of the actual NPM detectors in terms of light output and pulse height resolution [10] with the introduction of substantial systematic errors in the unfolding [11].

2.3.2. Unfolding

A two-components model was used in the unfolding to describe neutrons produced by D ions in thermal equilibrium (TH component) and neutrons due to reactions involving supra-thermal ions (NTH component). The spectral components due to neutrons scattered in the tokamak structures (background) and to 14 MeV neutrons due to triton burn-up were not modelled. A Gaussian model (defined by width, i.e. temperature T, average energy ($\langle E \rangle$) and amplitude (A)) was adopted both for TH and NTH2 and the simultaneous unfolding of both components was performed under the following assumptions:

a) T_{TH} in the range 1-10keV. The 1keV lower limit is chosen since the achievable energy resolution at 2.5MeV, ~3.5% (i.e. ~20% of the pulse height resolution [10] (~17.6% in our case)), is approximately equal to the broadening (FWHM/$\langle E \rangle$) of a Gaussian neutron spectrum with TTH=1keV; any reconstructed TTH value below 1keV is considered as not reliable. An upper limit TTH=10 keV has been set, well above the value measured by the TOFOR spectrometer.
b) T_{NTH} (NTH component effective temperature) $\geq$ 10keV.
c) $\langle E \rangle_{TH} = \langle E \rangle_{NTH} = \langle E \rangle$ in the range 2-3MeV; $\langle E \rangle$ is left as a free parameter to accommodate for shifts in the reconstructed average energy due to mismatches between the simulated RF and the actual response of each detector.

The comparison between measured and folded PHS was restricted to the region between 0.6MeV_{ee} and 0.9MeV_{ee} in order to minimize the contamination due to g-rays and background (at lower energies)

[2] *Use of a Gaussian model for the non-thermal component of the neutron spectrum is strictly valid only for spectra due to non-thermal ions that have lost their anisotropy because of large pitch angle scattering occurring during their slowing down in the plasma.*

and to exclude regions with low statistics (at higher energies). Moreover, the PHS were roughly corrected for the contribution due to 14MeV neutrons by subtracting the average PHS counts in the region between 3 MeV_{ee} and 6 MeV_{ee}.

3. RESULTS

The typical output of the unfolding procedure is outlined in figure 2 for the NPM LOS (#14 vertical camera) that best matches the TOFOR LOS: the unfolded TH and NTH spectral components together with the measured PHS and the folded PHS are shown. The line-integrated ion temperature derived from unfolding ($T_{TH} = 6.8 \pm 0.5$keV) is consistent with TOFOR [8]; the effective temperature of the non-thermal component ($T_{NTH} = 43 \pm 4$keV) also agrees with the value obtained by fitting the TOFOR non-thermal component with a Gaussian function ($T_{NTH\ TOFOR} \sim 45$keV). The NPM temperature errors describe only the statistical part of the error (1s error on the fitted parameter) and not include any systematic contribution.

Figure 3 shows, for all NPM LOS, the folded PHS counts (C_n) in the range 0.6 MeV_{ee} - 0.9 MeV_{ee} and their breakdown into TH and NTH contributions; the thermal fraction ($C_{nTH}/(C_{nTH} + C_{nNTH})$) is also shown. Results indicate a strong decrease of the thermal fraction towards the plasma edge, in qualitative agreement with theoretical predictions [12]. Note that the thermal fraction for LOS #14 (61.6%) is consistent with the TOFOR value.

Figure 4 shows the profile of the line-integrated TNTH and TTH obtained from the unfolding of all NPM LOS. The T_{NTH} is well in excess of 10 keV in all cases (typically $T_{NTH} \sim 35$keV, except for edge LOS #8, 9, 10 and 19 having implausibly higher values). The TTH of the vertical LOS are compatible with expectations, with higher values in the center and lower in the edge. The T_{TH} of the horizontal LOS (except for # 4 and #5) are equal either to the lower or upper boundary fixed for the fitting (the lower boundary is also hit by vertical LOS #11, #18 and #19). Apart from the unsuitability of the simple two-Gaussian model and inappropriateness of the simulated RF, the T_{NTH} and T_{TH} values of the edge LOS suffer from low statistics (see Fig.3) as well as backscattering effects [1]. Moreover, the determination of T_{TH} may also fail in some cases due to the fact that non-thermal component >> thermal component. However, the data and analysis procedure appear strong enough to distinguish between the TH and NTH components.

Finally, the local ion temperature profile (T_i) obtained from the spatial inversion of the vertical NPM line-integrated spectra (excluding points with T_{TH} at fitting boundary values) is reported in figure 5 and compared with the electron temperature profile (Te) from Thomson Scattering (TSC) and the T_i profile from Charge Exchange Recombination Spectroscopy (CXRS). A rough agreement between the NPM and CXRS T_i profiles is observed up to mid-radius, while a discrepancy appears for $r/a > 0.5$ ($T_{i\ NPM} < T_{i\ CXRS}$) due the limited number of edge LOS employed in the spatial inversion.

CONCLUSIONS

The present analysis shows that the JET NPM upgraded with digital electronics can provide, through the measurement of the neutron pulse height spectra for each LOS, information on the profiles of the ion temperature and the relative contribution to the neutron emission of the thermal and non-thermal ion components. The results encourage further enhancements such as the use of

LED correction systems and the measurement of the response functions for each detector in order to reduce the present large uncertainties in these measurements. Moreover, in future work, a more detailed modeling of the non-thermal neutron spectra can additionally provide spatially-resolved information on the fast ion velocity distribution functions.

ACKNOWLEDGEMENTS

This work was supported by EURATOM and carried out within the framework of the European Fusion Development Agreement. The views and opinions expressed herein do not necessarily reflect those of the European Commission.

REFERENCES

[1]. J.M. Adams et al., NIM A 329, 277 (1993).
[2]. J.M. Adams and G. White, NIM 459, 156 (1978).
[3]. M. Riva et al., Fusion Engineering and Design **86**, 1191 (2011).
[4]. D. Marocco et al., Nuclear Fusion **51**, 053011 (2011).
[5]. A. Zimbal et al., Review of Scientific Instruments **75**, 3553 (2004).
[6]. D. Marocco et al., IEEE Transactions on Nuclear Science **56**, 1168 (2009).
[7]. M. Riva et al., Fusion Engineering and Design **82**, 1245 (2007).
[8]. C. Hellesen et al., Review of Scientific Instruments **81**, 10D337 (2010).
[9]. G. Dietze and H. Klein, PTB Report PTB-ND-22, ISSN 0572 (1982).
[10]. H. Klein, S. Neumann, NIM A 476 132 (2002).
[11]. A. Zimbal, private communication (2012).
[12]. O.N. Jarvis, Plasma Physics and Controlled Fusion **39**, 1571 (1997).

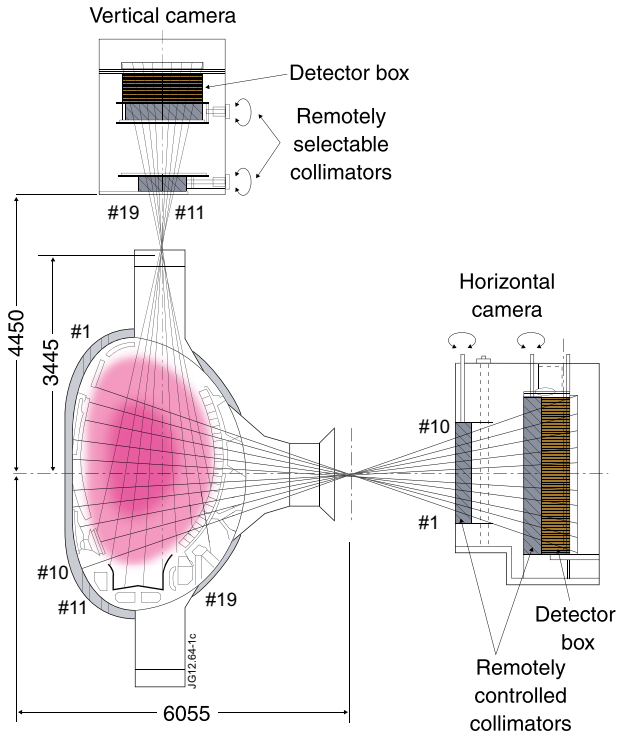

Figure 1: Neutron profile monitor layout.

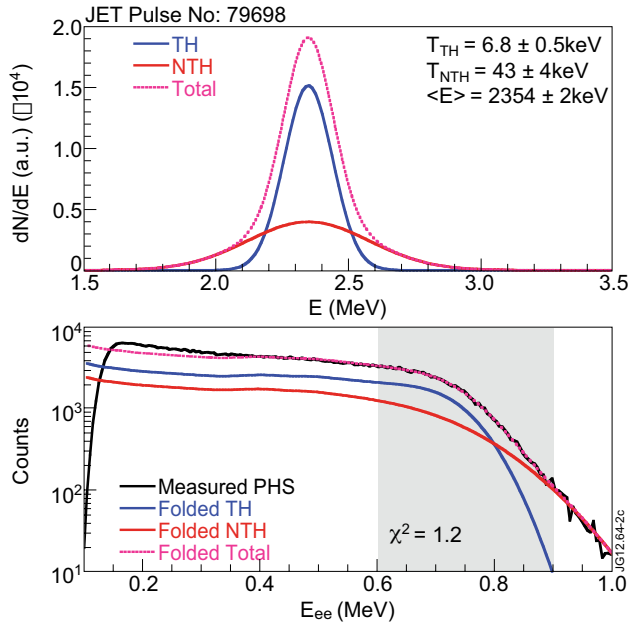

Figure 2: JETPulse No: 79698 (time window 12-16s) - NPM LOS # 14: unfolded TH and NTH neutron spectra components (top); measured and folded PHS with breakdown in TH and NTH contributions (bottom); the shaded area locates the energy region used for the unfolding.

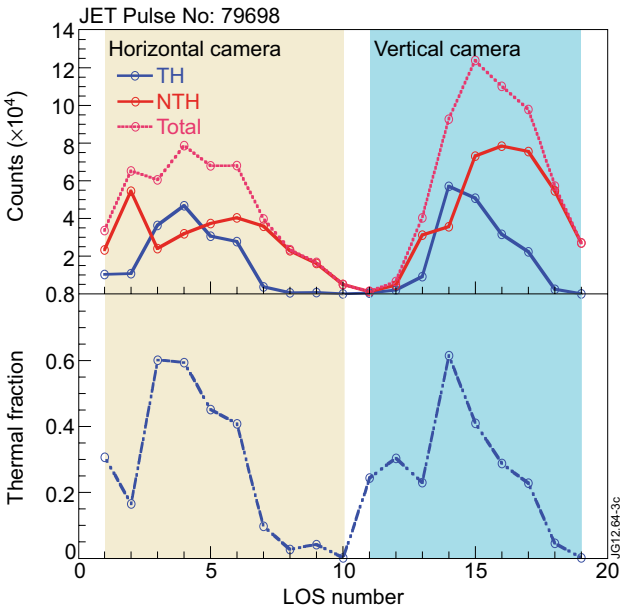

Figure 3: JETPulse No: 79698: folded PHS counts between 0.6 MeV_{ee} - 0.9 MeV_{ee} (top) and thermal fraction (bottom) as a function of NPM LOS number.

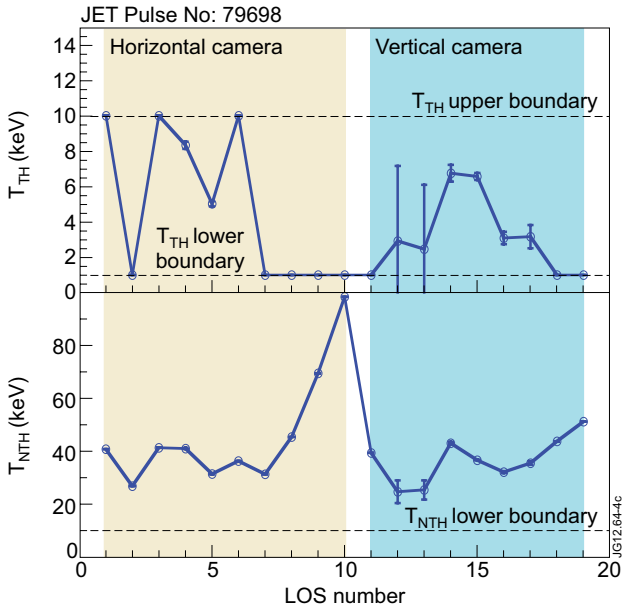

Figure 4: JETPulse No: 79698: Line-integrated T_{TH} and T_{NTH} as a function of NPM LOS number.

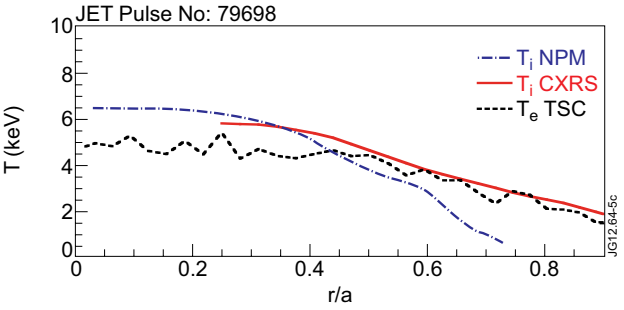

Figure 5: JET Pulse No: 79698: comparison between T_i from NPM and CXRS and T_e from TSC.